Intermetalloid Clusters

DOI: 10.1002/anie.201005655

$[Eu@Sn_6Bi_8]^{4-}$: A Mini-Fullerane-Type Zintl Anion Containing a Lanthanide Ion**

*Felicitas Lips, Rodolphe Clérac, and Stefanie Dehnen**

In memory of Hans Georg von Schnering

Experimental and theoretical studies on intermetalloid cluster anions,[1] that is, main-group-element cages with interstitial transition metal atom(s), have attracted the interest of chemists and physicists for about a decade. This is due to a large variety of novel structural types, unprecedented bonding situations, and unexpected chemical and physical properties of the resulting phases; furthermore, the compounds are discussed as being models for doped materials and/or precursors to novel intermetallic phases.[2] The structures of the known intermetalloid anions are controlled by both the synthetic reaction route and the embedded transition metal atom. For instance, whereas most of the reports include closed-shell d^{10} metal atoms, two of the most recent results showed that endohedral Group 8 or Group 9 metal atoms serve to stabilize small non-deltahedral clusters $[Fe@Ge_{10}]^{3-}$ [3] and $[Co@Ge_{10}]^{3-}$,[4] that would not exist without interstitial atom. These anions feature exclusively non-deltahedra faces and thus direct toward fullerene-like molecular structures.[2a]

To date, it has not been possible to isolate main-group-metal cages stabilized by Ln ions, although these elements are well-known as both components of intermetallic phases, for example, in $EuSn_3Sb_4$,[5] and as guests in doped main-group-element host lattices, for example in nanocrystalline LED phosphors such as $M_2Si_5N_8:Eu^{2+}$ (M = Sr, Ba)[6] or laser materials such as Nd:YAG.[7] Moreover, photoelectron spectroscopy[8] and quantum chemical investigations[9] indicated the existence of $[LnSi_n]^-$ species ($3 \le n \le 13$; Ln = Ho, Gd, Pr, Sm, Eu, Yb), $[EuSi_n]^-$ ($3 \le n \le 17$), and $Yb@Pb_{12}$ in the gas phase. In the condensed phase, Ln ions have only been trapped by carbon cages such as $M@C_{82}$ and $M_2@C_x$ (M = La–Nd, Sm–Lu; $x = 72, 78, 80$).[10] These clusters have been discussed as "designer" materials because a small variation in their composition can significantly manipulate their chemical, electronic, and magnetic properties. For instance, the magnetic moment is tunable by the type and oxidation state of the incorporated lanthanide ion.[8]

We have extended our recent investigations of compounds comprising ternary Zintl anions, such as $[K([2.2.2]crypt)]_4[Zn@Zn_5Sn_3Bi_3@Bi_5]\cdot 0.5en\cdot 0.5tol$ (en = 1,2-ethylenediamine, tol = toluene),[11] formed upon reactions of the binary precursor $[Sn_2Bi_2]^{2-}$ [12] by the introduction of a lanthanide ion, which gave rise for the formation of a spherical cluster with a fullerene-related structure: The reaction of $[K([2.2.2]crypt)]_2[Sn_2Bi_2]\cdot en$ with $[(C_5Me_4H)_3Eu]$ yields the desired compound $[K([2.2.2]crypt)]_4[Eu@Sn_6Bi_8]\cdot 1.1en$ (**1**) as extremely air-sensitive, dark brown crystals (yield: 11% with respect to $[Sn_2Bi_2]^{2-}$) along with the crystalline starting material (>80%; see the Supporting Information).

Six Sn and eight Bi atoms in the $[Eu@Sn_6Bi_8]^{4-}$ anion in **1** (Figure 1) form a polyhedron that consists of nine non-deltahedral faces, namely six pentagons and three square faces. This enneahedron has been unknown to date in an isolated, ligand-free form. However, topologically identical polyhedra were previously observed and discussed as part of complicated networks within two solid-state phases: elongated in the intermetallic phase Ag_7Te_4[13] or undistorted in

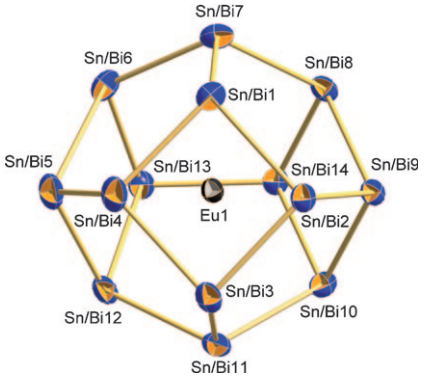

Figure 1. View of the $[Eu@Sn_6Bi_8]^{4-}$ anion in **1**. Orange/blue spheres denote Sn/Bi mixed sites with site occupation factors of 0.76–0.11 (Sn) and 0.24–0.89 (Bi). Selected bond lengths [Å]: Sn/Bi–Sn/Bi 2.8297(11)–3.0393(9); Sn/Bi–Eu 3.3515(8)–3.5770(9).

[*] F. Lips, Prof. Dr. S. Dehnen
Fachbereich Chemie and Wissenschaftliches Zentrum für Materialwissenschaften, Philipps-Universität Marburg
Hans-Meerwein-Strasse, 35032 Marburg (Germany)
Fax: (+49) 6421-282-5653
E-mail: dehnen@chemie.uni-marburg.de
Homepage: http://www.uni-marburg.de/fb15/ag-dehnen
Prof. Dr. R. Clérac
CNRS, UPR 8641, Centre de Recherche Paul Pascal (CRPP)
Equipe "Matériaux Moléculaires Magnétiques"
115 avenue du Dr. Albert Schweitzer, Pessac 33600 (France)
and
Université de Bordeaux, UPR 8641, Pessac 33600 (France)

[**] This work was supported by the Fonds der Chemischen Industrie FCI (Chemiefonds-Stipendium for F.L.), the Deutsche Forschungsgemeinschaft (DFG), the University of Bordeaux, the Région Aquitaine, GIS Advanced Materials in Aquitaine (COMET Project), and the CNRS. We are grateful to Dr. U. Linne and J. Bamberger for ESI-MS measurements.

Supporting information for this article is available on the WWW under http://dx.doi.org/10.1002/anie.201005655.

the Zintl phase $Na_{29}Zn_{24}Sn_{32}$ as $[Na@Sn_{14}]$.[14] The latter, which is linked to other structural units, represents the homometallic analogue of the anion of **1** (see below).

Disregarding the distribution of the Sn or Bi atoms, the cluster topology represents a flattened sphere of idealized D_{3h} symmetry, with the Eu atom located almost perfectly on the geometric barycenter of the 14-atom cage. Three square faces (Sn/Bi1–4, Sn/Bi5,6,12,13, and Sn/Bi 8–10,14) surround the cluster equator, being linked by E–E contacts (E = Sn/Bi) along an equatorial ring. The two hemispheres are capped by the two poles of the cluster anion (Sn/Bi7 and Sn/Bi11), completing three pentagons that meet there.

The use of binary precursors allows an optimization of the total electron number of the resulting anion during its formation and crystallization, and therefore proved to be a very useful synthetic tool.[11,15] However, whereas the charge of the anion in **1** is unambiguous according to the number of four $[K([2.2.2]crypt)]^+$ counterions per cluster anion, heavy statistical and/or rotational disorder of the two different main-group elements hampered a trivial assignment of Sn and Bi atomic positions. This problem is known to be intrinsic for Group 14/15 Zintl ions,[11,12] and is more serious with an increasingly spherical shape of the cluster. Here, the ratio Eu/Sn/Bi = 1:6:8 in the crystalline compound was experimentally determined by electrospray ionization mass spectrometry (ESI-MS; Figure 2) of single crystals dissolved in dimethylformamide, energy dispersive X-ray (EDX) analysis, and thorough X-ray structure refinement using second free variables. The ESI-MS investigations indicate a very complicated, possibly dynamic, situation upon re-dissolvation of the crystals, at least under ESI-MS conditions. However, the spectrum that is obtained immediately upon injection of the freshly prepared solution (Supporting Information, Figure S4) shows only a few fragments beside the molecular peak.

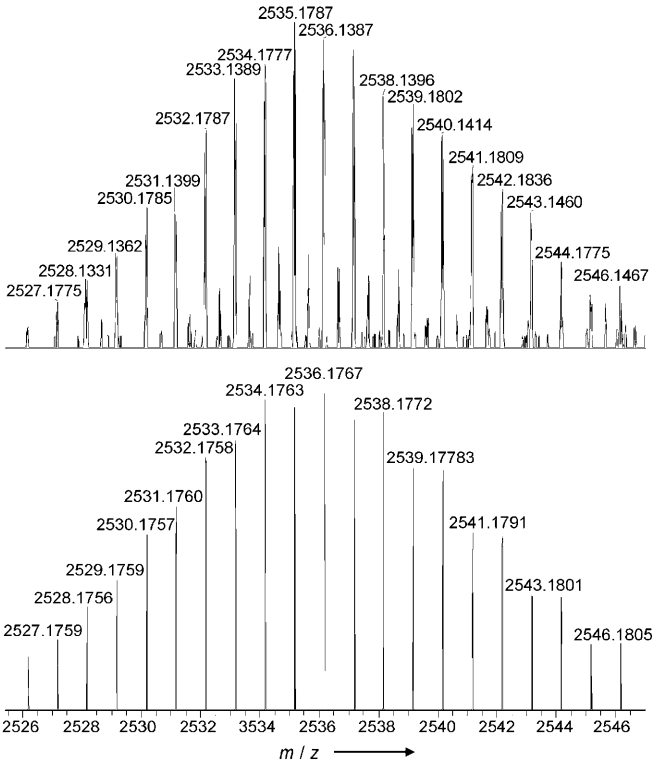

Figure 2. Negative-ion ESI mass spectrum of **1**. The spectrum shows the oxidized $[Eu@Sn_6Bi_8]^-$ ion measured (top) and calculated (bottom). For further details, see the Supporting Information.

The anion composition that was determined from these experiments would still allow for two different situations, considering the formal oxidation state of the interstitial Eu atom and accordingly the charge and electronic situation of the $[Sn_6Bi_8]$ shell: a) Eu^{III} in $[Eu^{3+}@(Sn_6Bi_8)^{7-}]^{4-}$, according to the $[(C_5Me_4H)_3Eu^{III}]$ starting material, or b) Eu^{II} in $[Eu^{2+}@(Sn_6Bi_8)^{6-}]^{4-}$ upon reduction of the Ln ion under the prevailing highly basic and reductive reaction conditions. As outlined in the following, experimental and quantum chemical investigations of the magnetism and also topology studies in comparison with the reported 14-atom enneahedra helped to rationalize case (b) as being the one observed in the title compound.

Both cases add up to an odd total electron number of $(1\times63)+(6\times4)+(8\times5)=127$, thus producing a paramagnetic species. However, whereas Eu^{III} usually adopts a diamagnetic ground state, Eu^{II} is expected to exist in the stable $S=7/2$ high-spin state. Thus, the first case, $[Eu^{3+}@(Sn_6Bi_8)^{7-}]^{4-}$, should result in an $S=1/2$ ground state owing to the odd electron number within the 14-atom cage, whilst the second case, $[Eu^{2+}@(Sn_6Bi_8)^{6-}]^{4-}$, is expected to produce a significantly larger spin ground state. Magnetic measurements were performed on polycrystalline samples of **1**. Due to the extremely air-sensitive nature of the compound and co-crystallization of the diamagnetic starting materials that are almost impossible to separate from **1**, several measurements on different batches resulting from different "selections" of crystals were carried out and compared (Supporting Information, Figure S2). The temperature dependence of the susceptibility for the different batches is globally identical, showing a Curie–Weiss paramagnetic behavior. Due to the presence of diamagnetic impurities, the Curie constant increases from 1.2 to 5.3 $cm^3\,K\,mol^{-1}$ upon a better separation of **1** from its starting materials. These results established unambiguously a spin ground state for **1** that is higher than $S=5/2$ (as a maximum Curie constant of 4.375 $cm^3\,K\,mol^{-1}$ is expected for $S=5/2$) and definitely precludes an $S=1/2$ ground state. On the batch that displays the highest Curie constant, that is, the batch with the highest content of **1** obtained by hand separation, magnetization measurements were performed between 1.8 and 8 K. Although an $S=5/2$ Brillouin function is not able to satisfactory fit the data, an $S=7/2$ Brillouin function (55 % of $S=7/2$ with $g=2$) reproduces almost perfectly the experimental data, further supporting an $S=7/2$ ground state for **1** (Supporting Information, Figure S3). Furthermore, it is worth mentioning that the positive Weiss constant (+0.2 K) is obtained for this batch, which suggests the presence of ferromagnetic interactions between $S=7/2$ $[Eu@Sn_6Bi_8]^{4-}$ spin carriers in the crystal lattice.

The magnetic properties of **1** are in agreement with comprehensive quantum chemical investigations, using density functional theory (DFT)[16] methods of the RIDFT program[17] within the program system TURBOMOLE.[18]

These results clearly favor the high-spin $S = 7/2$ ground state over $S = 1/2$ for all of the investigated $[Eu@Sn_6Bi_8]^{4-}$ isomers by at least 426 kJ mol^{-1} (see Supporting Information), whereas the calculation of intermediate spin states $S = 3/2$ or 5/2 did not lead to energy convergence in any of the investigated cases.

The assignment of a Eu^{II} ion leads to the formulation of a diamagnetic $[Sn_6Bi_8]^{6-}$ shell with eight three-connected Group 15 atoms beside six three-connected pseudo Group 15 atoms. The respective electron count is identical to that of the homoatomic homologue reported for $Na_{29}Zn_{24}Sn_{32}$, where the $[Na@Sn_{14}]$ units are linked to the intermetallic framework by eight covalent bonds, producing eight four-connected Group 14 atoms (with five valence electrons when additionally considering the external bond electrons) and six formally charged, three-connected pseudo Group 15 atoms. Therefore, the electron-precise situation in both systems leads to perfect agreement with the simple Zintl–Klemm–Busmann pseudo element concept.[19] In contrast to most of the known endohedral Zintl anions, there is no need to form a deltahedral cage to handle an electron deficit according to Wade–Mingos rules.[20] The formal +II oxidation state at the interstitial atom is further supported by the same situation being observed in $Eu@C_{82}$, for example.[21] Other Ln ions, such as La and Ce, encapsulated in this carbon cage prefer the trivalent state.[10]

With exclusively non-deltahedral faces, the structural features of the anion in **1** are related to those of fullerenes.[22] Therefore, DFT investigations were performed on a hypothetic C_{14} fullerene and the fully hydrogenated species $C_{14}H_{14}$. Investigation of the C_{14} cage, starting out from the given topology, shows that the C_{14} cage would undergo distinct structural changes due to steric strain (Figure 3a). In contrast,

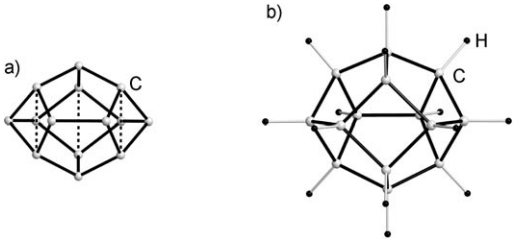

Figure 3. Structures of the hypothetical fullerene C_{14} (a) and its hypothetic, fully hydrogenated fullerane derivative $C_{14}H_{14}$ (b), resulting from geometry optimizations using DFT methods. C–C bond lengths [Å]: C_{14} 1.440–1.483 (dashed: 1.798). $C_{14}H_{14}$ 1.532–1.565.

the exclusively σ-bonded species $C_{14}H_{14}$ (Figure 3b), a so-called "fullerane"[23] that would be isoelectronic to a neutral $(E^{15})_{14}$ cage or an $[E^{14}{}_6E^{15}{}_8]^{6-}$ mixed element anion as in **1**, converges to exactly the observed topology (E^{14}, E^{15} = Group 14 or Group 15 element, respectively).

Only a few examples of purely inorganic fullerene-like or "fullerane"-like metal clusters have been isolated to date. One example is included in a network: the Zintl phase $Na_{96}In_{97}M_2$ (M = Ni, Pd, Pt)[24] comprises metal clusters In_{74} and $In_{48}Na_{12}$ as analogues to C_{74} and C_{60}.[25] A discrete cluster with a fully inorganic fullerene-like structural motif was realized with the 90-atom core in $[\{Cp^*Fe(\eta^5{:}\eta^1{:}\eta^1{:}\eta^1{:}\eta^1{:}\eta^1\text{-}P_5)\}_{12}\{CuCl\}_{10}\{Cu_2Cl_3\}_5\{Cu(CH_3CN)_2\}_5]$.[26] The onion-type cluster anion $[As@Ni_{12}@As_{20}]^{3-}$[27] comprises an As_{20} fullerane-type dodecahedron, which represents a Group 15 analogue of the smallest known fullerene C_{20}.[28] Among the large number of metalloid aluminum and gallium clusters with metal–metal bonds,[29] $[Al_{50}(Cp^*_{12})]$[30] possesses a pseudo fullerene carbon shell protecting an Al_{50} cluster core. A 14-atom cage that is structurally closely related to the anion in **1** was observed in $[Ge_{14}\{Ge(SiMe_3)_3\}_5Li_3(thf)_6]$.[31] However, here the six Ge atoms without $Ge(SiMe_3)_3$ ligands or charge, which only comprise four valence electrons, form additional Ge–Ge bonds, similar to the above-mentioned interaction of the six equatorial carbon atoms in C_{14}.

DFT investigations of the ternary anion in **1** have been useful to suggest the most probable $[Sn_6Bi_8]$ atomic distribution within the 14-atom shell and to identify stability criteria for the latter. For this, different $[Sn_6Bi_8]$ atomic distributions in the anion of **1** were calculated (all with the preferred $S = 7/2$ ground state). The examples were selected out of a total of 293 isomers, according to representative structural features (see Supporting Information). The result clearly showed that the length of Sn_x chains ($x = 0$–6) within the $[Sn_6Bi_8]$ cluster surface and their spatial distribution seems to be the most significant parameter for the stability of the intermetalloid cluster anion: isomers with isolated tin atoms and a single Sn–Sn dumbbell turned out to be the most stable forms (Figure 4). This is most probably due to a preference to

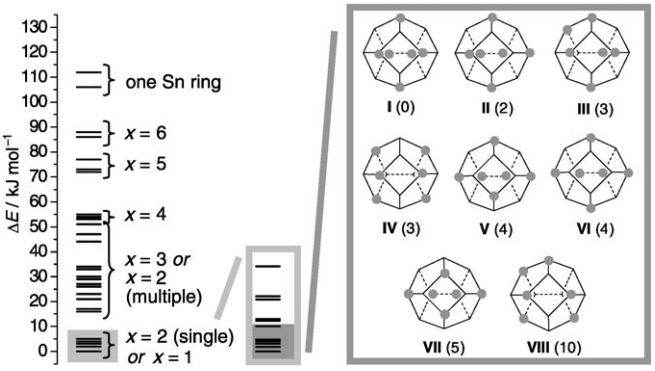

Figure 4. Relative DFT energies ΔE of selected isomers of $[Eu@Sn_6Bi_8]^{4-}$ with respect to the most stable isomer; *x* denotes the length of the longest Sn_x chain present on the $[Sn_6Bi_8]$ surface of the ternary anion. The eight isomers of lowest energy (**I**–**VIII**) are drawn schematically (without the interstitial Eu atom), together with the respective value of ΔE; gray spheres represent Sn atoms.

maximize the number of heteroatomic Sn–Bi bonds, additionally taking into account suitable positions of the atoms; the latter favors the larger Bi atoms on the positions with most acute angles, that is, directly beside the pole positions (Σ303.18–304.71°), whereas poles (Σ316.39, 316.57°) and equatorial positions (Σ305.71–312.22°) are rather occupied by Sn atoms. These demands led to a shortlist of 13 isomers exhibiting the most likely positions of Sn and Bi atoms in $[Eu@Sn_6Bi_8]^{4-}$. Eight of these isomers show energy differences within the error of the quantum chemical method;

therefore the observed anion in **1** might represent one, or a statistical mixture of these (Figure 4). The most stable form, conformer **I**, shows similar positions of the Bi atoms as found for the four-connected Sn atoms in the Sn_{14} polyhedron in $Na_{29}Zn_{24}Sn_{32}$. However, owing to additional restrictions within the solid-state framework, the latter favors the more symmetric arrangement of the six three-connected Sn atoms as three Sn–Sn dumbbells along the cluster equator, which is disfavored by 26 kJ mol^{-1} here (see the Supporting Information).

Formation mechanisms of intermetalloid cluster anions are widely unknown to date. However, ESI-MS investigations of the reaction mixture gives some indication for the formation of **1**. The mass spectra reveal several $[Sn_xBi_y]$ fragments ($x+y=3$–9; see Supporting Information) to result from decomposition/re-arrangement of the starting compound $[Sn_2Bi_2]^{2-}$, producing nine-atom cages as atom-consuming major side-products, which is common for this type of reaction.[11] One fragment of low intensity accords to the composition $[Sn_3Bi_4]^-$ (Figure 5a), which is anticipated to

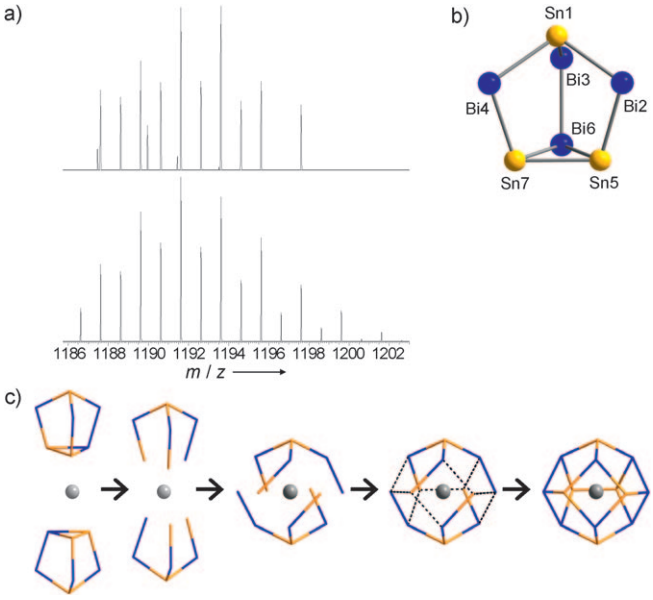

Figure 5. a) ESI mass spectrum of the fragment $[Sn_3Bi_4]^-$, measured (top) and calculated (bottom) and b) calculated minimum structure. c) Hypothetical growing pathway of $[Eu@Sn_6Bi_8]^{4-}$ out of two hemispheres that derive from $[Sn_3Bi_4]^{6-}$ nortricyclane-type cages.

represent a nortricyclane-type $[Sn_3Bi_4]^{6-}$ cage in solution, typical for seven-atom Zintl anions. A homologous cage, $[Sn_3Sb_4]^{6-}$, was previously isolated as $[K_6(NH_3)_9][Sn_3Sb_4]$.[15]

DFT calculations of $[Sn_3Bi_4]^{6-}$ resulted in convergence for all 10 possible isomers (see Supporting Information), with the lowest-energy isomer (Figure 5b) representing exactly the topology of a hemisphere of the lowest-energy structure of the cluster (conformer **I** in Figure 4). This fragment, together with its low abundance, might give a hint for the growing pathway of the observed, low-yield enneahedron in **1**, out of two seven-atom hemispheres. A hypothetical reaction pathway (Figure 5c) should include redox processes that lead to opening of the nortricyclane-type cages and endohedral trapping of the reduced Eu ion, followed by the fusion of the fragments into the observed final composition of the $[Eu@Sn_6Bi_8]^{4-}$ anion in **1**. We assume that the Eu ion adopts the role of a template, allowing only for the selective formation and crystallization of the cluster anion in **1**.

Quantum-chemical investigations served to explore how the interstitial Eu atom interacts with the binary cage, by means of a Mulliken population analysis[32] of the most stable isomer **I**. Although 6s, 5d, and 4f atomic orbitals (AOs) of the Eu atom do contribute to molecular orbitals (MOs) that comprise contributions from (mainly) p-AOs of both Sn and Bi atoms, the low percentage of the Eu contributions (7–11%) indicate that covalent bonding does not play a significant role for the Eu–Sn/Bi contacts. Figure 6 shows

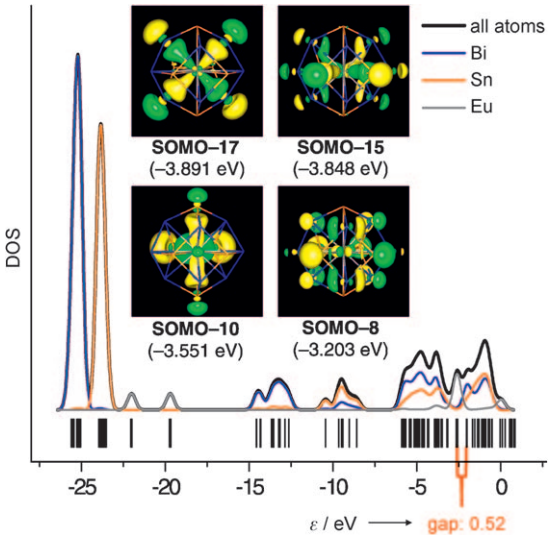

Figure 6. Molecular-orbital energy scheme of the valence-orbital region and calculated density of states (DOS) of $[Eu@Sn_6Bi_8]^{4-}$; selected Eu–Sn/Bi bonding MOs and according orbital energies ε (in brackets) with highest Eu d AO contributions (SOMO–17: 9%, SOMO–15: 10%, SOMO–10: 11%) and highest Eu 4f contribution (SOMO–8 7%), along with contributions of Sn and Bi atoms. Electron densities are drawn to 0.2 e$^-$ Å^{-3} (for further details, see the Supporting Information).

the density of states (DOS) of the $[Eu@Sn_6Bi_8]^{4-}$ anion for all atoms and for the different atom types as well as the four Eu–Sn/Bi bonding MOs with the highest Eu AO contributions to the intermetallic interaction.

The DOS diagram confirms a clear separation into MOs with Eu contributions and MOs with Sn and Bi contributions in the frontier-orbital region. The rather ionic nature of the embedded atom, which was also observed for the non-deltahedral examples $[M@Ge_{10}]^{3-}$ (M = Fe, Co) mentioned above,[3,4] correlates well with the electron-precise anionic main-group-element cage and seems to be the reason for the observed structural features. The relatively small SOMO–LUMO gap (0.52 eV; SOMO = (highest) singly occupied molecular orbital; LUMO = lowest unoccupied molecular orbital) results from the high orbital energy of the singly

occupied Eu 4f AOs, whereas the energy difference of 1.12 eV between the highest-occupied MOs with Sn/Bi contribution (SOMO−7) and the LUMO indicates a semimetallic situation within the Sn/Bi cage of the anion, a situation similar to doped semimetals.

In conclusion, the results discussed herein shed light on the novel class of intermetalloid cluster compounds containing lanthanide ions that open up a new direction toward innumerable further examples with original electronic and/or magnetic properties.

Experimental Section

All details on the synthesis of **1**, single-crystal X-ray diffraction, energy-dispersive X-ray analysis, electrospray ionization mass spectrometry, SQUID measurements, and quantum-chemical investigations are provided in the Supporting Information. CCDC 783141 (**1**) contains the supplementary crystallographic data for this paper. These data can be obtained free of charge from The Cambridge Crystallographic Data Centre via www.ccdc.cam.ac.uk/data_request/cif.

Received: September 9, 2010
Published online: December 9, 2010

Keywords: bismuth · europium · intermetalloid clusters · tin · Zintl anions

[1] a) T. F. Fässler, S. D. Hoffmann, *Angew. Chem.* **2004**, *116*, 6400 – 6406; *Angew. Chem. Int. Ed.* **2004**, *43*, 6242 – 6247; b) S. C. Sevov, J. M. Goicoechea, *Organometallics* **2006**, *25*, 5678 – 5692; c) S. Scharfe, T. F. Fässler, *Philos. Trans. R. Soc. London Ser. A* **2010**, *368*, 1265 – 1284. The term "intermetalloid cluster" for endohedral Zintl anions was introduced by Fässler et al. in Ref. [1a].

[2] a) N. Korber, *Angew. Chem.* **2009**, *121*, 3262 – 3264; *Angew. Chem. Int. Ed.* **2009**, *48*, 3216 – 3217; b) T. F. Fässler, *Angew. Chem.* **2007**, *119*, 2624 – 2628; *Angew. Chem. Int. Ed.* **2007**, *46*, 2572 – 2575.

[3] B. Zhou, M. S. Denning, D. L. Kays, J. M. Goicoechea, *J. Am. Chem. Soc.* **2009**, *131*, 2802 – 2803.

[4] J.-Q. Wang, S. Stegmaier, T. F. Fässler, *Angew. Chem.* **2009**, *121*, 2032 – 2036; *Angew. Chem. Int. Ed.* **2009**, *48*, 1998 – 2002.

[5] R. Lam, J. Zhang, A. Mar, *J. Solid State Chem.* **2000**, *150*, 371 – 376.

[6] M. Zeuner, P. J. Schmidt, W. Schnick, *Chem. Mater.* **2009**, *21*, 2467 – 2473.

[7] J. E. Geusic, H. M. Marcos, L. G. Van Uitert, *Appl. Phys. Lett.* **1964**, *4*, 182 – 184.

[8] a) A. Grubisic, Y. J. Ko, H. Wang, K. H. Bowen, *J. Am. Chem. Soc.* **2009**, *131*, 10783 – 10790; b) A. Grubisic, Y. J. Ko, H. Wang, K. H. Bowen, *J. Chem. Phys.* **2008**, *129*, 054302.

[9] J. P. Dognon, C. Clavaguéra, P. Pyykkö, *Angew. Chem.* **2007**, *119*, 1449 – 1452; *Angew. Chem. Int. Ed.* **2007**, *46*, 1427 – 1430.

[10] H. Shinohara, *Rep. Prog. Phys.* **2000**, *63*, 843 – 892.

[11] F. Lips, S. Dehnen, *Angew. Chem.* **2009**, *121*, 6557 – 6560; *Angew. Chem. Int. Ed.* **2009**, *48*, 6435 – 6438; [2.2.2]crypt: 4,7,13,16,21,24-hexaoxa-1,10-diazabicyclo[8.8.8]hexacosane.

[12] S. C. Critchlow, J. D. Corbett, *Inorg. Chem.* **1982**, *21*, 3286 – 3290.

[13] R. M. Imamov, Z. G. Pinsker, *Kristallografiya* **1966**, *11*, 182 – 190. Ag_7Te_4 comprises interconnected chains of $[Ag_{12}Te_2]$ units that share a common Te atom along the crystallographic *c* axis. However, the topological analogy to the anion in **1** is much smaller than it is the case for $Na_{29}Zn_{24}Sn_{32}$, as the electronic situation is rather different here. All atoms possess large coordination numbers (6 or 8), and the $[Ag_{12}Te_2]$ cages are elongated along the pseudo-C_3 axis with respect to that observed in **1**, producing two triangles instead of square faces; the most significant common feature is thus the existence of the 14-atom cavity. A fragment of the structure is shown in the Supporting Information, Figure S23.

[14] S.-J. Kim, S. D. Hoffmann, T. F. Fässler, *Angew. Chem.* **2007**, *119*, 3205 – 3209; *Angew. Chem. Int. Ed.* **2007**, *46*, 3144 – 3148.

[15] F. Lips, I. Schellenberg, R. Pöttgen, S. Dehnen, *Chem. Eur. J.* **2009**, *15*, 12968 – 12973.

[16] R. G. Parr, W. Yang, *Density Functional Theory of Atoms and Molecules*, Oxford University Press, New York, **1988**.

[17] a) K. Eichkorn, O. Treutler, H. Öhm, M. Häser, R. Ahlrichs, *Chem. Phys. Lett.* **1995**, *242*, 652 – 660; b) K. Eichkorn, F. Weigend, O. Treutler, R. Ahlrichs, *Theor. Chem. Acc.* **1997**, *97*, 119 – 124.

[18] R. Ahlrichs, M. Bär, M. Häser, H. Horn, C. Kölmel, *Chem. Phys. Lett.* **1989**, *162*, 165 – 169.

[19] *Chemistry, Structure and Bonding of Zintl Phases and Ions: Selected Topics and Recent Advances* (Ed.: S. M. Kauzlarich), VCH, New York, **1996**.

[20] a) K. Wade, *Adv. Inorg. Chem. Radiochem.* **1976**, *18*, 1 – 67; b) D. M. P. Mingos, *Nature Phys. Sci.* **1972**, *236*, 99 – 102; c) D. M. P. Mingos, *Acc. Chem. Res.* **1984**, *17*, 311 – 319.

[21] B.-Y. Sun, T. Sugai, E. Nishibori, K. Iwata, M. Sakata, M. Takata, H. Shinohara, *Angew. Chem.* **2005**, *117*, 4644 – 4647; *Angew. Chem. Int. Ed.* **2005**, *44*, 4568 – 4571.

[22] The analogy of purely inorganic, anionic cages to fullerenes was previously also discussed more generally for deltahedral cluster anions. See, for example: a) T. F. Fässler, *Angew. Chem.* **2001**, *113*, 4289 – 4293; *Angew. Chem. Int. Ed.* **2001**, *40*, 4161 – 4165; b) Ref [1a]; c) L.-F. Cui, X. Huang, L.-M. Wang, J. Li, L.-S. Wang, *Angew. Chem.* **2007**, *119*, 756 – 759; *Angew. Chem. Int. Ed.* **2007**, *46*, 742 – 745.

[23] R. Nesper, *Angew. Chem.* **1994**, *106*, 891 – 894; *Angew. Chem. Int. Ed. Engl.* **1994**, *33*, 843 – 846.

[24] S. C. Sevov, J. D. Corbett, *Science* **1993**, *262*, 880 – 883.

[25] P. W. Fowler, D. E. Manolopoulos, *An Atlas of Fullerenes*, Clarendon Press, Oxford, **1995**.

[26] J. Bai, A. V. Virovets, M. Scheer, *Science* **2003**, *300*, 781 – 783.

[27] M. J. Moses, J. C. Fettinger, B. W. Eichhorn, *Science* **2003**, *300*, 778 – 780.

[28] H. Prinzbach, A. Weiler, P. Landenberger, F. Wahl, J. Wörth, L. T. Scott, M. Gelmont, D. Olevano, B. von Ossendorff, *Nature* **2000**, *407*, 60 – 63.

[29] a) A. Ecker, E. Weckert, H. Schnöckel, *Nature* **1997**, *387*, 379 – 381; b) A. Schnepf, H. Schnöckel, *Angew. Chem.* **2001**, *113*, 733 – 737; *Angew. Chem. Int. Ed.* **2001**, *40*, 711 – 715.

[30] J. Vollet, J. R. Hartig, H. Schnöckel, *Angew. Chem.* **2004**, *116*, 3248 – 3252; *Angew. Chem. Int. Ed.* **2004**, *43*, 3186 – 3189.

[31] C. Schenk, A. Schnepf, *Chem. Commun.* **2008**, 4643 – 4645.

[32] R. S. Mulliken, *J. Chem. Phys.* **1955**, *23*, 1833 – 1840.

